Project ID: **65422**

Project Title: **Modeling of Spinel Settling in Waste Glass Melter**

Lead Principal Investigator:

Dr Pavel R. Hrma
Staff Scientist
Pacific Northwest National Laboratory
MSIN K6-24
P. O. Box 999
Richland, Washington 99352
Telephone: 509-376-5092
e-mail: pavel.hrma@pnl.gov

Co Principal Investigators:

Dr. Lubomir Nemec
Institute of Inorganic Chemistry
Czech Academy of Sciences
Prague Czech Republic
Czech Republic
Telephone: +420-2-24-310-371
e-mail: nemec@uach.iic.cas.cz

Dr. Petr Schill
Glass Service, Ltd.
75501
Vsetin Czech Republic
Czech Republic
Telephone: +420-657-611-439
e-mail:research@gsl.cz

Modeling of Spinel Settling in Waste Glass Melter

(First Year of Funding: FY 1998)

Principal Investigator

Dr. Pavel Hrma
Pacific Northwest National Laboratory
P.O. Box 999, MSIN K6-24
Richland, WA 99352
(509) 376-5092 (phone)
(509) 372-0682 (fax)
pavel.hrma@pnl.gov

Co-Principal Investigator

Dr. Petr Schill
Glass Service, Ltd.
Vsetin, Czech Republic
+420-657-611-439 (phone)
+420-657-611-430 (fax)
research@gsl.cz

University Collaborators

Professor Lubomir Nemec
Institute of Inorganic Chemistry
Czech Academy of Sciences
Prague, Czech Republic
+420-2-24-310-371 (phone)
nemec@uach.iic.cas.cz

Dr. Martin Mika
Institute of Chemical Technology
Prague, Czech Republic
martin.mika@vscht.cz

Dr. Jaroslav Klouzek
Institute of Chemical Technology
Prague, Czech Republic
jaroslav.klouzek@vscht.cz

Contributors

Pavel Izak (Post Master Research Associate)
Trevor Plaster (Undergraduate Student Fellow)

Research Objective

Each 1% increase of waste loading (W), defined as the high-level waste (HLW) mass fraction in glass, can save the U.S. Department of Energy (DOE) over a half billion U.S. dollars for vitrification and disposal. For a majority of Hanford and Savannah River waste streams, W is limited by spinel precipitation and settling in waste glass melters. Therefore, a fundamental understanding of spinel behavior is crucial for economy and the low-risk operation of HLW vitrification.

The goal of this research is to develop a basic understanding of the dynamics of spinel formation and motion in velocity, temperature, and redox fields that are characteristic for the glass-melting process. This goal is being achieved by directly studying spinel formation and settling in molten glass and by developing a mathematical tool for predicting the spinel behavior and accumulation rate in the melter.

The main potential benefit of this study is achieving a lower waste-glass volume, which translates into a shorter cleanup time, a smaller processing facility, a smaller repository space, and, hence, a reduced investment of time and money to reach acceptable technical risks. Additional benefits include 1) more accurately assessing sensible limits for problem constituents (such as chromium) in the melter feed, 2) reducing the blending requirements, and 3) comparing cost and risk with other options (pretreatment, blending or diluting the waste) to determine the best path forward. The results of this study will allow alternate melter designs and operating conditions to be evaluated. The study will also address the option of removing the settled sludge from the melter.

Problem Statement

Accumulation of insoluble phases interferes with melter operation and shortens melter lifetime. The current HLW vitrification strategy is to minimize insoluble phases and to avoid crystallization in the melter by imposing on glass formulation the requirement that the liquidus temperature (T_L) is below the minimum temperature of the glass in the melter (T_L <1050°C). This restriction avoids the risk of spinel formation in the melter at a very high cost. An adequate constraint of crystallization behavior of HLW glass may result in an increase of W by several mass per cents.

This project is generating essential thermodynamic, kinetic, hydrodynamic, and rheological data to assess the rate that spinel forms and settles. These data include physical and geometric parameters of the melter, glass properties, spinel equilibria in HLW glass, spinel crystallization kinetics, the rate of spinel settling in high-viscosity melts (subjected to complex velocity, temperature, and redox fields), and the rheological characteristics of spinel sludge in molten glass. The rate of spinel settling and accumulation on the melter bottom will be estimated using mathematical modeling. In addition, the study will address spinel formation during the melter feed reactions, spinel agglomeration, and spinel interaction with gas bubbles.

Research Progress and Implications

Melter Selection

The slurry-fed ceramic melter (SFCM) designed and operated at Pacific Northwest National Laboratory (PNNL) (Goles and Nakaoka 1990) was selected for the modeling work.

Glass Selection

Based on previous studies (Mika et al. 1997, Hrma et al. 1999), nine glasses were formulated with different content of spinel-forming oxides (NiO, Cr_2O_3, Fe_2O_3, and MnO). Glass compositions and their liquidus temperatures (T_L) are listed in Table 1.

Table 1. Compositions (in Mass Fractions), Estimated Viscosity, and Measured T_L of Glasses

	MS-1	MS-2	MS-3	MS-4	MS-5	MS-6	MS-7	MS-8	MS-9
Al_2O_3	0.080	0.080	0.080	0.080	0.080	0.0800	0.0800	0.0800	0.0800
B_2O_3	0.070	0.070	0.070	0.070	0.070	0.0700	0.0700	0.0700	0.0700
Cr_2O_3	0.007	0.005	0.005	0.005	0.005	0.0035	0.0030	0.0035	0.0100
Fe_2O_3	0.130	0.145	0.115	0.089	0.115	0.1250	0.1150	0.1250	0.1100
Li_2O	0.045	0.040	0.040	0.045	0.041	0.0300	0.0454	0.0300	0.0400
MgO	0.006	0.006	0.006	0.006	0.006	0.0060	0.0060	0.0060	0.0060
MnO	0.005	0.005	0.005	0.005	0.005	0.0036	0.0050	0.0036	0.0036
Na_2O	0.157	0.153	0.153	0.153	0.153	0.1573	0.1530	0.1573	0.1573
NiO	0.020	0.012	0.012	0.012	0.007	0.0140	0.0095	0.0075	0.0100
SiO_2	0.450	0.424	0.454	0.475	0.458	0.4600	0.4531	0.4600	0.4531
ZrO_2	0.030	0.060	0.060	0.060	0.060	0.0506	0.0600	0.0571	0.06
η (Pa·s)[(a)]	4.19	4.10	5.37	5.37	5.37	7.62	4.43	7.62	5.08
T_L (°C)[(b)]	1247	1215	1185	1139	1171	1225	1114	1125	1199
T_L (°C)[(c)]	1221	1223	1188	1144					

(a) Estimated value at 1150°C.
(b) Measured value at PNNL.
(c) Measured value at the Institute of Chemical Technology, Prague.

MS-4 glass was chosen as an internal standard for T_L. MS-7 and MS–9 glasses are used as model glasses for this study.

Glass and Spinel Properties

The viscosity (η) data of MS-7 glass and electrical conductivity (ε) data for MS-7 and MS-9 glasses are listed in Table 2. Viscosity versus temperature for MS-7 glass has been fitted as $\ln(\eta) = -6.00155 + 6072/(540.9 + T)$. The specific heats of molten glasses measured by a differential scanning calorimeter (DSC) within the temperature interval from 850°C to 1250°C are $c_p = 1.35\ J \cdot g^{-1} \cdot K^{-1}$ for MS-7 glass and

$c_p = 1.860 - 1.00\times10^{-4}T - 1.508\times10^{5}T^{-2}$ (T is in K) for MS-9 glass. The preliminary estimate for the effective heat conductivity of MS glasses at 1150°C is $k_{ef} = 3.31\ W\cdot m^{-1}\cdot K^{-1}$. This estimate is based on measured values for welding glasses with a similar iron content.

Table 2. Viscosity Data for MS-7 Glass and Electrical Conductivity Data for MS-7 and MS-9 Glasses

MS-7				MS-9	
T (°C)	η (Pa·s)	T (°C)	ε (S/m)	T (°C)	ε (S/m)
1251	1.14	1245	67.87	1250	62.14
1210	1.59	1206	59.98	1201	54.97
1171	2.11	1157	51.89	1152	47.30
1140	2.67	1109	44.17	1104	40.02
1094	3.76	1059	36.80	1055	33.29
1049	5.93	1011	30.13	1006	27.19
1000	9.83	963	24.04	958	21.70
950	17.78	913	18.59	908	16.72
902	35.81	864	13.80	859	12.51
853	79.78				

Spinel was separated from SS-AA glass designed to produce a large fraction of spinel while the glass was sufficiently fluid to allow settling. SS-AA glass composition in mass% oxides is SiO_2 44.94, B_2O_3 6.84, Na_2O 15.37, Li_2O 2.93, MgO 2.11, Al_2O_3 7.82, Fe_2O_3 14.93, Cr_2O_3 1.50, MnO 0.35, and NiO 3.21. This glass was heated for five days at 1100°C to generate spinel sludge for rheological studies and for isolating spinel. To separate spinel, the solid sludge was dissolved in HNO_3 at 60°C for four days. A magnet was used to remove spinel from the residue. The density of this spinel was estimated from the x-ray diffraction (XRD)-lattice parameters to be 5.1 to 5.2 $g\cdot cm^{-3}$; its volume expansion coefficient is approximately $6.5\times10^{-5}\ K^{-1}$. Spinel composition was measured indirectly by calibrated scanning electron microcopy with energy-dispersive spectroscopy (SEM-EDS), and directly by separating spinel from the glass and using energy dispersive x-ray fluorescence (EDXRF).

Spinel Equilibria

The effect of the concentration of spinel-forming components in glass on the equilibrium fraction of spinel is shown in Figure 1. The effect of HLW components on T_L with the spinel primary phase is shown in Table 3 (Hrma et al. 1999).

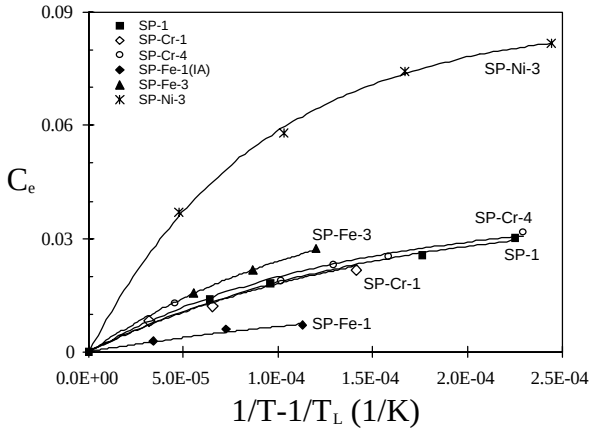

Figure 1. Equilibrium Fractions of Spinel in the Baseline Glass SP-1 and Glasses with Varied Spinel-Forming Components Displayed as a Function of Temperature (Stachnik and Hrma 1999). The content of spinel-forming oxides (in mass%) was Cr_2O_3 0.22, NiO 0.52, and Fe_2O_3 12.50 in SP1; Cr_2O_3 0.00 in SP-Cr-1 and 1.20 in SP-Cr-4; NiO 3.00 in SP-Cr-3; Fe_2O_3 6.00 in SP-Fe-1 and 15.00 in SP-Fe3. The remaining components were in the same proportions as in SP-1.

Table 3. Partial Specific T_L Values (T_{Li}) for Glass Components (in °C)

Al_2O_3	B_2O_3	CaO	Cr_2O_3	Fe_2O_3	K_2O	Li2O	MgO	MnO	Na_2O	NiO	SiO_2	TiO_2	U_3O_8	Others
2866	403	1757	20592	2685	-980	-1367	3820	1312	-1736	9530	1010	4925	1633	3583

The spinel equilibrium fraction (C_e) is measured by heat-treating the glass long enough at a constant temperature to reach equilibrium, quenching the melt and using quantitative XRD. The results are checked by optical microscopy with an image analyzer. Spinel equilibrium as a function of temperature can be fitted by the equation (Reynolds and Hrma 1997)

$$C_e = C_{\max}\left\{1-\exp\left[-B_L\left(\frac{1}{T}-\frac{1}{T_L}\right)\right]\right\} \tag{1}$$

where $C_{\max}$, and B_L are composition-dependent coefficients.

Spinel Precipitation Kinetics

Reynolds and Hrma (1997) have shown that spinel nucleates readily, without a measurable incubation period, and crystallizes rapidly (Figure 2). Spinel crystallization kinetics can be represented by the equation

$$\frac{dC}{dt} = nk(C_e - C)\left[-\ln\left(1-\frac{C}{C_e}\right)\right]^{(n-1)/n} \tag{2}$$

where C is the spinel fraction in molten glass, n the Avrami number, the value of which is n = 1.5 for spinel crystallization in a HLW borosilicate glass and

$$k = k_0 \exp\left(-\frac{B_k}{T}\right) \tag{3}$$

is the crystallization rate coefficient; k_0, and B_k are composition-dependent coefficients. Equation (2) can be solved for a T = constant to yield the Kolmogorov-Mehl-Avrami-Johnson equation:

$$C = C_e\left\{1-\exp\left[-(kt)^n\right]\right\} \tag{4}$$

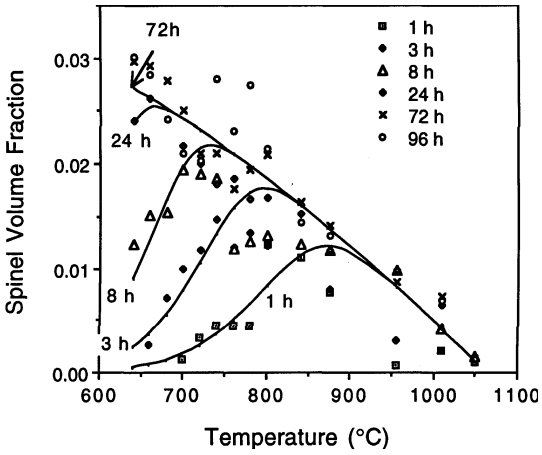

Figure 2. Volume Fraction of Spinel Precipitated from a HLW Glass under Isothermal Conditions as a Function of Temperature and Time (Reynolds and Hrma 1997)

For spinel formation under a more complex temperature history, Equation (2) needs to be verified. Casler and Hrma (1999) made the first step in this direction by solving Equation (2) for a constant rate of cooling and for the temperature history typical for a HLW glass canister.

The dependence of the equilibrium and kinetic coefficients, i.e., C_{max}, B_L, k_0, and B_k, on glass composition provides an opportunity for optimization guided by mathematical modeling. This dependence is most conveniently represented by partial specific coefficients defined by the equation (Hrma 1998)

$$P = \sum_{i=1}^{N} P_i g_i \tag{5}$$

where P is a composition-dependent coefficient, P_i is the i-th component partial specific coefficient (also called component coefficient), g_i is the i-th component mass fraction in glass, and N is the number of the key components. Composition coefficients for T_L are listed in Table 3.

The composition effects (including glass redox) on spinel equilibrium and the rate of crystallization in MS-7 glass are being measured as a function of temperature. We use ultraviolet-visible-near infrared (UV-VIS-NIR) and Mössbauer spectroscopy to measure the iron redox ratio in glass and spinel. To control the oxygen pressure, we equilibrate glass with CO/CO_2 atmosphere.

Spinel Dissolution Kinetics

Spinel forms during the batch melting reactions, dissolves as temperature increases, and precipitates again as the melt temperature decreases below T_L. The spinel dissolution rate determines how much, if any, of the original spinel survives in the stream of molten glass and subsequently grows at colder sections of the melter. Because spinel dissolution occurs near T_L, where glass has a low viscosity, settling of crystals interferes with the measurement. The same is true about crystallization kinetics near T_L. Preparations for the dissolution study are in progress.

Spinel Formation in the Cold Cap

Melting reactions in HLW glass batches were investigated previously (Anderson et al. 1994a, b; Smith et al. 1995; Vienna et al. 1999). However, little is known about spinel formation during the initial melting reactions. A quantitative description of spinel formation during melting reactions is needed for

realistic modeling. Spinel formation during the batch melting reactions is being investigated using a time-temperature function that is close to the temperature history of feed within the cold cap.

Melter feed slurries were prepared for MS-7 and MS-9 glasses. Spinel-forming components in the form of Fe, Ni, Cr, and Mn nitrates were dissolved in deionized water and co-precipitated by mixing the solution with enough 10 M NaOH at 40°C to supply the Na_2O of the glass. Other feed components, $ZrO(NO_3)_2 \cdot 2H_2O$, $Mg(NO_3)_2 \cdot 6H_2O$, Li_2CO_3, SiO_2 sand (• 190 µm), Al_2O_3, and H_3BO_3 were stirred into the co-precipitate to prepare the slurry feed. The slurry was dried in an oven at 90°C for two days. Approximately 1.3-g samples were ramp-heated in platinum crucibles at 4°C/min starting from 200°C. Crucibles were removed from the furnace at different temperatures, quenched, and analyzed by XRD and SEM.

The semi-quantitative mass fractions of crystalline phases in MS-7 glass are plotted against temperature in Figure 3. Nitrates decomposed and quartz dissolved by 750°C. Spinel appeared above 400°C, peaked at 650°C, and dissolved by 1150°C. A yellow-green chromate melt occurred at 700°C to 900°C. Feed volume increased several times at temperatures above 700°C and collapsed at above 900°C. Interestingly, carnegieite was observed above 700°C and persisted up to 1150°C. The work is ongoing.

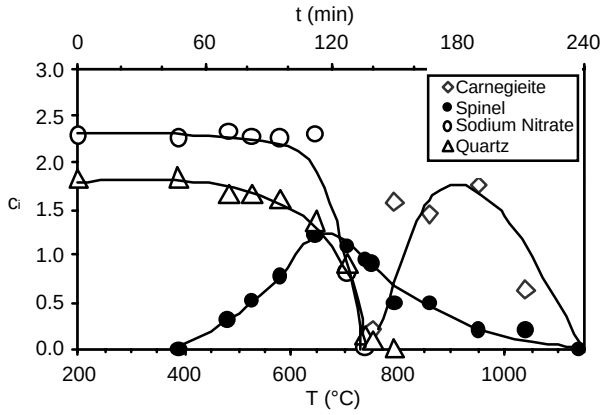

Figure 3. Evolution of Crystalline Phases During Ramp Heating of MS-7 Glass Feed (c_i is crystal fraction in mass%)

Spinel Agglomeration and interaction with Gas Bubbles

Agglomeration and interaction with bubbles may influence spinel settling in melters. LaMont and Hrma (1998) observed these phenomena in laboratory crucibles. Spinel agglomerates by the shear flocculation mechanism in steep velocity (Cobb and Hrma 1991, LaMont and Hrma 1998, Schweiger et al. 1998). LaMont and Hrma (1998) observed the interaction of spinel with bubbles in silica crucibles as a result of silica dissolution in the melt. Evidence exists (Kim and Hrma 1994) that a large concentration of bubbles produced by redox reactions affects the melt flow under the cold cap. Mathematical modeling of the redox field will show the degree to which bubbles and spinel can interact within the melter.

Spinel Settling

The hydrodynamics of spinel settling in a high-viscosity liquid entails a two-phase mixture of spinel and molten glass. LaMont and Hrma (1998) have shown that spinel particles in molten glass behave as a swarm rather than individual bodies even when their concentration is low and distances between them are large. Spinel settling produced a single flow-cell within the crucible, indicating that in a larger volume of melt, a cellular convection pattern will probably evolve.

We conducted preliminary experiments with corundum particles suspended in a model liquid of the same viscosity as molten glass. The suspension was dyed and placed on top of pure model liquid. Settling was recorded by camera (Figure 4). The corundum particles did not settle individually; the suspension plunged into the less dense liquid below. The maximum velocity, measured at the tip of the plume, was nearly time-independent and increased nearly linearly with corundum concentration (Figure 5). These results will be used for model verification.

Mathematical Model

Mathematical modeling adopted in this study is based on a numerical solution of field equations on a system of three-dimensional discrete grids by the control-volume method that enables proper balances of all quantities. We modified the glass model code to accept specific features of the SFCM geometry, the slurry and cold cap regions, the electrode arrangement, special input and output, and material properties. After tuning, the code was modified to incorporate density variation caused by spinel and to describe spinel settling. The first stage of the project is focused on mathematical simulation of the temperature, electric, and velocity fields in the melt and the cold-cap of a test SFCM under various operation conditions. This simulation is based on literature data and PNNL staff communication (Peters et al. 1990; Goles and Nakaoka 1990).

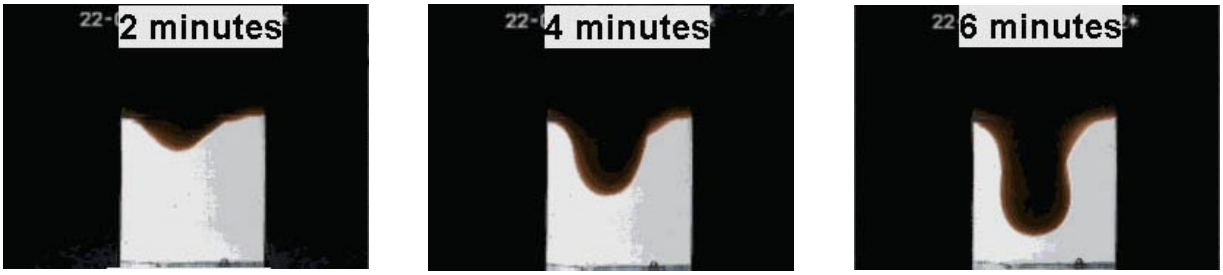

Figure 4. Motion of the Boundary between the Liquid with Suspended Corundum Particles (10 µm, 5 g·m^{-3}) and the Pure Liquid

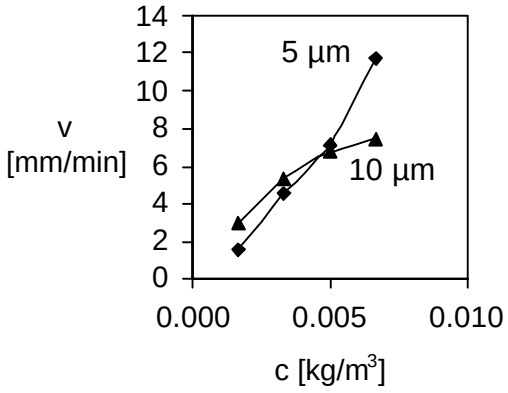

Figure 5. The Settling Velocity Versus Corundum Concentration

The glass model code was adapted to 1) accept a batch blanket composed from two parts (the slurry pool and the cold cap), 2) approximate the plenum space, and 3) enable glass density dependence on other than temperature variables. The SFCM geometry was set up by the Glass Service GS-CAD program using PNNL blueprints. The model melter has the 0.79-m nominal glass depth, 2.0-m^2 surface area

(1.15×1.73 m), and 0.67-m plenum space height above the glass. Two electrode walls have a 30° slope, and the remaining two walls have a 66° slope against the horizontal level. The melt was Joule-heated by single-phase electric current from three submerged bock electrodes (Elliott et al. 1994).

The nonuniform net, automatically generated by the GS-CAD program, involved 79×91×84 grid nodes. Measured MS-7-glass properties were used when available; other melt properties (Table 4) were taken from the literature (Peters et al. 1990, Palmer 1991, Eyler et al. 1991). The batch-to-glass conversion degree was estimated from gradient-furnace experiments (Anderson et al. 1994a).

The operation parameters and boundary conditions were set up as follows (Peters et al. 1990; Palmer 1991; Choi 1991):

glass pull:	1080 kg/day
electrode voltage:	-56.8 V (bottom electrode), +28.4 V (side electrodes)
total electric supply:	96 kW
surface temperature:	900°C (glass), 100°C (slurry), 500°C (cold cap)
melter operating temperature:	1150°C

The Joule heat distribution (Figure 6, upper left) shows unusually high values in the middle-lower part and low values in the middle-upper part. This Joule heat distribution can by changed by modifying electrode voltages if necessary. The temperature and flow in both cuts (cross and longitudinal) show the good mixing ability of this type of melter.

Table 4. Glass Properties as Function of Temperature (in K)

Property	Formula
Density [kg/m^3]	$\rho(T) = 2497 - 0.2300T$
Kinematic Viscosity [m^2/s]	$\nu(T) = \exp[-20.02 + 19880/(4.663\times10^{-4} + T)]$
Specific Heat [J/(kg·K)]	$c = 2512$
Thermal Conductivity [W/(m·K)]	$\lambda(T) = 1.78 + 0.0004T$ at $300<T<1000$
	$\lambda(T) = 2.737 - 0.0024214T + 1.86384\times10^{-6}T^2$ at $1000<T<1800$
Electrical Conductivity [S/m]	$\sigma(T) = \exp[6.921 - 2844/(-475.0 + T)]$

For the spinel settling model, we treated spinel as a mixture component characterized by the pure-component density (ρ_0), particle diameter (d), and mass concentration (c). For spinel-melt interaction, we postulate the constitutive equation

$$F^g = -A(c,d)v^g\left(u^g - u\right) \tag{6}$$

where F^g is the force from particles to glass, υ^g is the liquid kinematic viscosity, u^g is the liquid velocity, u is the velocity of particles, and A is a coefficient that depends on c and d, such that A (0) = 0. For small c and d, $A = A_0cd$, where A_0 is a shape factor.

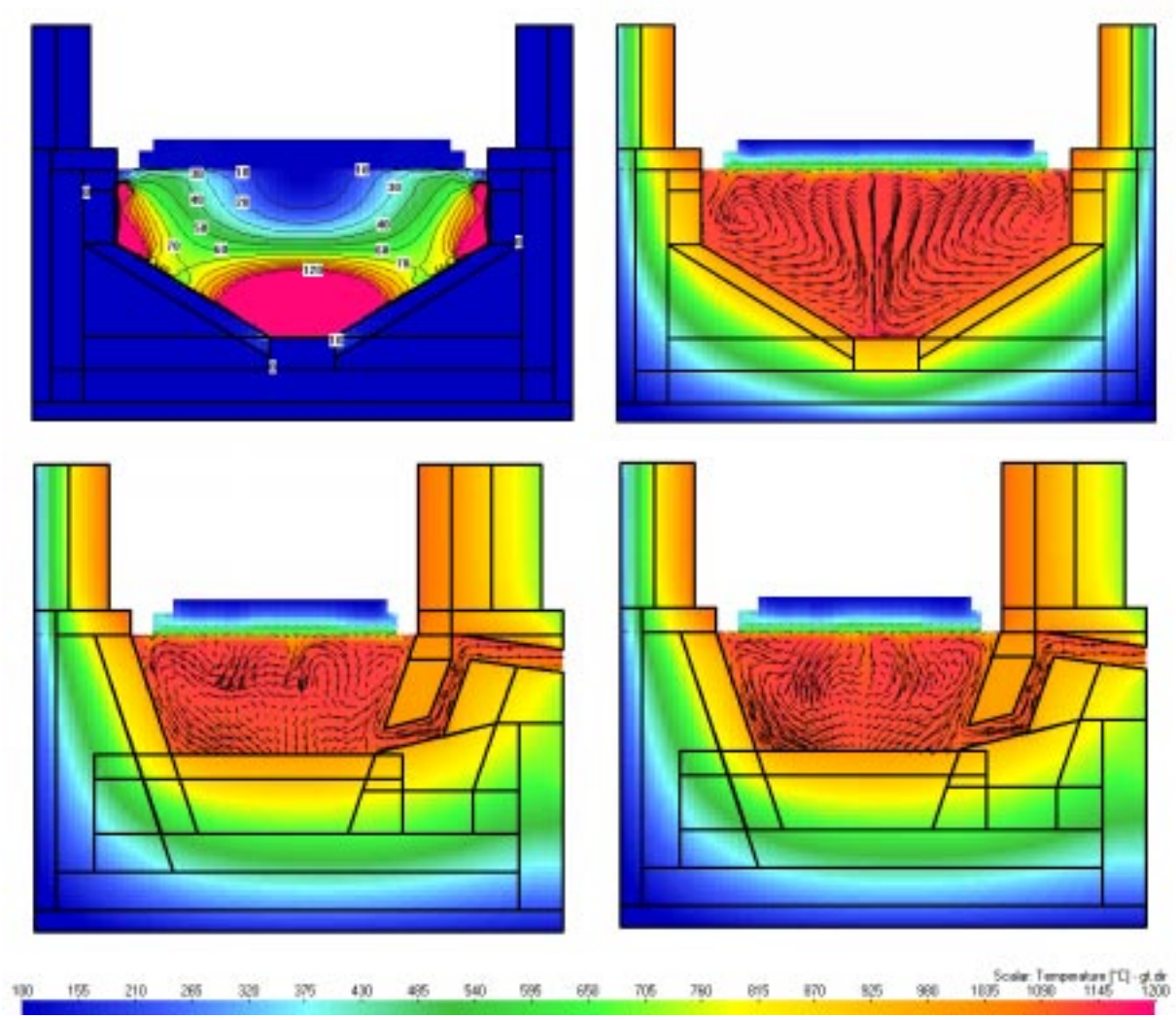

Figure 6. Examples of Electric (in kW/m^3), Temperature, and Flow Fields

We used the particle mass balance and the balance of force

$$u \cdot \nabla c = D\Delta c + E(c) \tag{7}$$

$$\frac{d}{dt}(cu) = -F^g + \frac{\pi}{6}(\rho^g - \rho)gd^3 \tag{8}$$

where D is the diffusion coefficient (estimated from the Stokes-Einstein equation), E(c) is the source term, and g is gravity. Equations (6) to (8) constitute the basis for modeling experiments, currently in progress.

Spinel Sludge Rheology

Spinel sludge was prepared by the method described above. Its behavior was tested using a rotatind spindle viscometer. Preliminary results indicate that spinel sludge behaves as a pseudoplastic rheopectic liquid.

Planned Activities

We will continue to measure the kinetics of spinel crystallization and dissolution under both isothermal and nonisothermal conditions and to evaluate component coefficients for spinel equilibrium and kinetics. The study of the redox effect on spinel formation will also continue.

We will study the spinel settling mode and rate in molten glass and also pay attention to spinel agglomeration and interaction with bubbles. We will finish the study of spinel sludge rheology as a function of temperature, shear rate, and aging. Physical modeling will be further developed to verify mathematical models.

The modified mathematical model will be used to predict the rate of spinel settling in the melter. A parametric study of mathematical simulation will be performed, focusing on identifying the potential for glass formulation optimization and melter design and operation optimization with respect to waste vitrification economy (maximum waste loading) and minimum risk (minimum spinel accumulation and melter disturbances).

References

Anderson LD, T Dennis, ML Elliott, and P Hrma. 1994a. "Waste glass melting stages." *Ceram. Trans*. 39:213-220.

Anderson LD, T Dennis, ML Elliott, and P Hrma. 1994b. "Noble metal behavior during melting of simulated high-level nuclear waste feeds." *Ceram. Trans*. 39:213-222.

Casler DG and P Hrma. 1999. "Nonisothermal kinetics of spinel crystallization in a HLW glass." *Scientific Basis for Nuclear Waste Management* (eds.), Material Research Society, Pittsburgh, Pennsylvania. (In print)

Choi IG. 1991. "Mathematical modeling of radioactive waste glass melter." *Ceram. Trans*. 23:385-394.

Cobb WT and P Hrma. 1991. "Behavior of RuO_2 in a glass melt." *Ceram. Trans*. 23:233-237.

Elliott ML, LL Eyler, LA Mahoney, MF Cooper, LD Whitney, and PJ Shafer. 1994. *Preliminary melter performance assessment report.* PNL-9822, Pacific Northwest Laboratory, Richland, Washington.

Eyler LL, ML Elliott, DL Lessor, and PS Lowery. 1991. "Computer modeling of ceramic melters to assess impacts of process and design variables on performance." *Ceram. Trans*. 23:395-407.

Goles RW, and RK Nakaoka. 1990. *Hanford Waste Vitrification Program Pilot-Scale Ceramic Melter*. PNL-7142, Pacific Northwest Laboratory, Richland, Washington.

Hrma P. 1998. "Empirical models and thermodynamic constitutive functions for high-level waste glass properties." *Ceram. Trans*. 87:245-252.

Hrma P, JD Vienna, M Mika, JV Crum, and GF Piepel. 1999. *Liquidus Temperature Data for DWPF Glass*. PNNL-11790, Pacific Northwest National Laboratory, Richland, Washington.

Kim DS and P Hrma. 1994. "Laboratory studies for estimation of melting rate in nuclear waste glass melters." *Ceram. Trans*. 45:409-419.

LaMont MJ and P Hrma. 1998. "A crucible study of spinel settling in a high-level waste glass." *Ceram. Trans*. 87:343-348.

Mika M, MJ Schweiger, and P Hrma. 1997. "Liquidus temperature of spinel precipitating high-level waste glass." WJ Gray and IR Triay (eds.), *Scientific Basis for Nuclear Waste Management*, 465:71-78, Material Research Society, Pittsburgh, Pennsylvania.

Palmer RA. 1991. "West Valley strategy for meeting waste acceptance preliminary specifications." *Ceram. Trans*. 23:475-490.

Peters RD, ML Elliott, and CC Chapman. 1990. "Proposed noble metals-compatible melter: Preliminary modeling results." *Ceram. Trans*. 9:567-580.

Reynolds JG and P Hrma. 1997. "The kinetics of spinel crystallization from a high-level waste glass." WJ Gray and IR Triay (eds.), *Scientific Basis for Nuclear Waste Management* 465:65-69, Material Research Society, Pittsburgh, Pennsylvania.

Schweiger MJ, MW Stachnik, and P Hrma. 1998. "West Valley high-level waste glass crystallization in canisters." *Ceram. Trans*. 87:335-341.

Smith PA, JD Vienna, and P Hrma. 1995. "The effect of melting reactions on laboratory-scale waste vitrification." *J. Mat. Res.*, 10[8]:2137-2149.

Stachnik MW, P Hrma, and H Li. 1999. "Effects of high-level waste glass composition on spinel precipitation." *Ceram. Trans*. 107 (to be published).

Vienna JD, DK Peeler, JG Darab, JR Zamecnik, H Li, and JE Mara. 1999. "Chemistry of rare earth oxalate vitrification" (to be published).

Publications and Presentations

Mika M, P Hrma, and MJ Schweiger. "Rheology of spinel sludge" (in preparation).

Stachnik MW, P Hrma, and H Li. 1999. "Effects of high-level waste glass composition on spinel precipitation." *Ceram. Trans*. 107 (to be published).

Izak P, P Hrma, and MJ Schweiger. "Nonisothermal crystallization of spinel from a high-level waste feed" (submitted to ACS 1999 meeting).

Hrma P, P Izak, J Klouzek, M Mika, L Nemec, and P Schill. "Chemistry and hydrodynamics of spinel settling in molten glass" (submitted to ACS 1999 meeting).

Schill P. "A three-dimensional mathematical model of radioactive waste glass melter" (submitted to ACS 1999 meeting).